UNIVERSITY OF TARTU
INSTITUTE OF ECOLOGY AND EARTH SCIENCES
DEPARTMENT OF GEOLOGY

Kaarel Mänd

Morphology and structure of putative fossilized phosphatic sulfur-bacteria and methanotrophic archea in 2.0 Ga old organic-rich mudstones, Zaonega formation

BSc thesis

Supervisor: Kalle Kirsimäe

TARTU 2013

Table of Contents

Introduction

Ca-phosphate in the form of apatite, is an important skeletal biomineral for several animal groups, such as brachiopods (e.g. Williams et al., 1992), conodonts (Ellison, 1944) and vertebrates (Ruben and Bennet, 1987). Apatite is also a common mineral phase replacing and therefore preserving organisms in the fossil record, which is known since Neoproterozoic (e.g. Cohen et al., 2011), whereas phosphatization is capable of preserving the most labile cellular tissues (Butterfield, 2003).

Marine phosphogenesis is widespread in the Phanerozoic (e.g. Föllmi, 1996), and the first sedimentary phosphatic deposits appear only in the Palaeoproterozoic as the direct consequence of the Great Oxygenation Event – GOE (Bekker et al., 2004; Nelson et al., 2010; Pufahl & Hiatt, 2012) that triggered continental (oxic) chemical weathering, delivery of increased phosphate to the oceans and higher bioproductivity as the result of that (Papineau, 2010; Pufhal & Hiatt, 2012).

One of the first phosphogenetic episodes of the Paleoproterozoic time occurs in 2.0 Ga old organic-rich mudstones and dolostones of the Zaonega Formation, Karelia, NW Russia (Lepland et al., 2013). Just recently Lepland et al. (submitted) suggested that the phosphate precipitation in Zaonega Formation was microbially induced and has preserved fossilized microbial consortia of methanotrophs and symbiotic sulfur oxidizing bacteria – dissolved phosphate secreting organisms that are also operating at sediment-water interfaces in modern times.

In modern seas the phosphorite precipitation occurs in areas characterized with high primary productivity at upwelling settings, such as those off Namibia (Föllmi, 1996; Schulz and Schulz, 2005), the Arabian Sea (Schenau et al., 2000) and the coast of Peru and Chile (Filippelli, 2011; Föllmi, 1996). Phosphate precipitation at anoxic-suboxic sediment-water interfaces in these areas is strongly bacterially mediated showing a close relationship between different groups of organisms, such as sulfide-oxidizing and sulfate reducing bacteria (Arning et al., 2008, 2009).

Giant sulfur-metabolizing bacteria are recognized as phosphate pre-concentrating/depositing organisms whose phosphate release rate under anoxic conditions and the phosphate-to-apatite conversion magnitude exceeds that during organic matter mineralization, and the mineralized phosphorous content in sediments associated with giant sulphide-oxidizing bacteria amounts

for 5% of dry sediment equivalent to 270 g of apatite per kg of sediment (Schulz and Schulz, 2005; Goldhammer et al., 2010; Brock and Schulz-Vogt, 2011).

Sulphide-oxidizing bacteria of genera *Thiomargarita* and *Beggiatoa* operate in close associations with methanotrophic archaea ANME-2 and ANME-1 habiting within microbial mats in modern venting areas (Knittel et al., 2005). Methanotrophic archea provide hydrogen sulfide as a by-product of anaerobic oxidation of methane that is used by sulfur-oxidizing microbial communities as an energy source (Knittel et al., 2005; Bailey et al., 2011).

Phosphate in Zaonega Formation sediments is commonly found in round-oval nodules with a mean diameter of a few to several hundred microns. In a smaller scale, the nodules and layers of apatite consist mainly of cylindrical particles with lengths of a few micrometers. The larger nodules were interpreted to be casts of sulfur-metabolizing bacteria and the smaller cylindrical particles resembled fossilized methanotrophic archea, which were thought to have colonized the cells and their surroundings after the environment became too sulfidic for the sulfur-metabolizers (Lepland et al., submitted).

Similarly the phosphatic nodules of about 500 μm in diameter are described in late Neoproterozoic Doushantuo Formation phosphorites, commonly regarded as fossilized eukaryotic embryos (Xiao et al., 1998). However, these finds have been controversially reinterpreted as *Thiomargarita* fossils based on similar shape, morphology and the diagenetic environment (Bailey, 2007).

Recognition of biogenicity of fossil structures, especially of Archean-Proterozoic putative microorganisms is not a straightforward task and a set of criteria has been developed to aid determination of the biological origin of fossil remains (e.g., Schopf and Walter, 1983, Buick, 1990; Schopf, 2004, 2005, 2007). A prime indicator of the biological origin of fossil-like objects is the micron-scale co-occurrence of identifiable biological morphology and geochemically altered remnants of biological chemistry. More specifically, the criteria include biologically plausible shapes and size distributions with distinct (carbonaceous) cell walls that define cell lumina. The specimens would be expected to occur in a biologically feasible environment in a multi-member population with numerous taxa present and that exhibit a plausible range of preservation types. The suspected mode of fossilization should be one that is previously documented for undoubtedly biological objects. Lastly, the putative fossils should exhibit a biological chemistry that is preserved as kerogen with isotopic compositions similar to those of biologically produced organic matter (Schopf et al., 2007).

However, the biological chemistry of the fossil remnants has the lowest preservation potential, especially when organic structures are replaced/mineralized. In this case the morphological criteria – size distribution, shape, structure, nature and diversity of preservational types – and the syngenetic environment are left for testing biogenity of putative organic structures.

In this thesis I study the phosphate occurrence in organic-rich mudstones and dolostones of the Zaonega Formation exposed at Shunga outcrop, Karelia. The objectives of this study are (a) to document the occurrence and size distribution of the microscopic apatitic nodules and cylinders; (b) to document the structure and recrystallization patterns of the cylinders and (c) to establish their biogenity and describe possible fossilization mechanisms.

Geological setting

Zaonega Formation is part of the Palaeoproterozic sedimentary succession, which occurs on the southeastern margin of the Fennoscandian (Baltic) Shield in NW Russia, central Karelia Onega Basin (Figure 1). The mixed volcanic-sedimentary sequence rests unconformably on Archean granites and gneisses. The Zaonega Formation fills a large NW-SE trending synform and dips 10-50°, diving under Palaeozoic platformal sediments to the south of the lake Onega. The Palaeoproterozoic sediments in the Onega Basin are divided into four groups – Sarioli, Jatuli, Ludikovi and Kalevi. During the Svecofennian orogeny 1.8 Gyr ago the succession was subjected to greenschist facies metamorphism (Melezhik et al., 1999, 2004; Ojakangas et al., 2001).
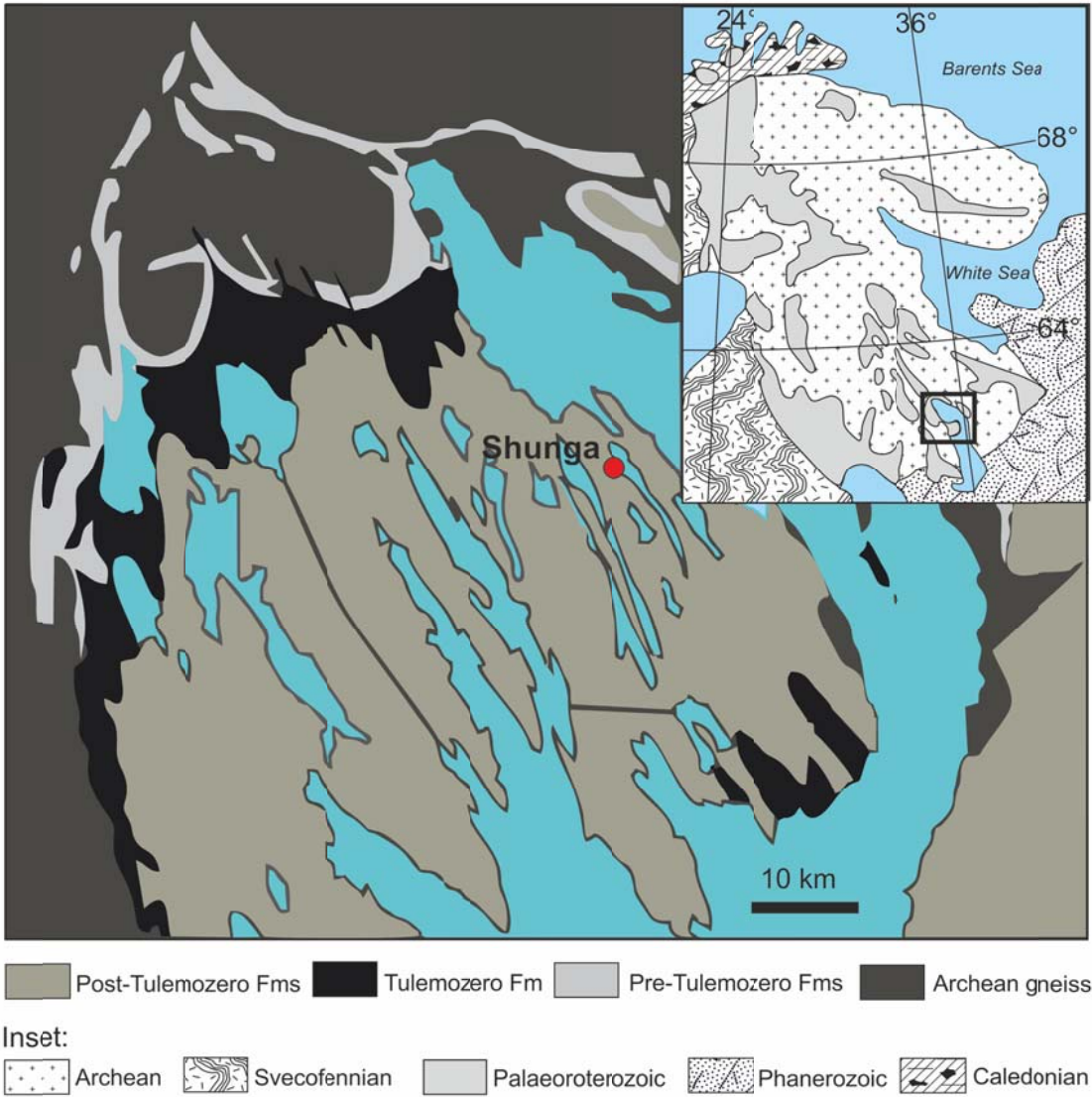

Figure 1: Geologic map of the Onega Basin, Karelia, Russia.

The ca. 1500-m thick Zaonega formation, which belongs in the Ludikovi group, is separated by an unconformity from the underlying Tulomozero Formation, while Suisari Formation basalts and gabbroic sills overlie it (Crne et al., 2013). Zaonega Formation is composed of mudstones, cherts and dolostones with abundant tuffs, lavas and sills intersecting or interlayering those. Most Zaonega Formation sedimentary rocks host at least several weight percent of organic carbon, with many highly-enriched layers which occasionally contain up to 98 wt.% (Melezhik et al., 1999).

Zaonega Formation is considered to be one of the richest accumulations of organic material reported from the Palaeoproterozoic and one of the first instances of petroleum generation in geologic history (Melezhik et al., 1999, 2004; Buseck, 1997). In some of these organic-rich layers in the upper part of the formation, there has been found elevated concentrations of phosphate (Crne et al., 2012; Lepland et al., submitted). The maximum age of 2090±70 Ma for Zaonega Formation is given by a Pb-Pb dating of the Tulomozero dolomites, whereas a Sm-Nd isochron dating from a gabbroic body intruding the Suisari formation provides the minimum age of 1980±27 Ma (Pukhtel et al., 1992).

Organic matter in the Zaonega formation is represented in an unusual form that has usually been termed shungite (after the village Shunga). Melezhik et al. (2004) describes it as "a black, non-crystalline, non-graphitised, structurally heterogeneous, glassy mineraloid with a semi-metallic lustre containing >98 wt.% C". Shungite can occur as autochtonous impregnations or as migrated bitumen in stratified organic-rich sediments and as organosiliceous material in diapiric deposits. The original depositional environment was lagoonal, brackish and non-euxinic (Melezhik et al., 1999, 2004). $\delta^{13}C$ values point to biogenic origin of the organic matter (Melezhik et al., 1999; Qu et al., 2012) which has been altered by later heavy diagenetic, catagenetic and metamorphic processes (Melezhik et al., 1999). Heat provided by the emplacement of sills into the carbonaceous sediments generated large amounts of petroleum, which then proceeded to migrate both horizontally and vertically, forming shungite deposits of concentrations higher than 50% (Melezhik et al., 2004).

The best known outcrop of shungite-bearing rocks is located near the Shunga village, in the northeastern part of the Onega structure, where this rock was mined in the 1930s (Figure 2) (Buseck, 1997; Melezhik et al., 1999). Its exact stratigraphic position is uncertain, but it is considered to represent the upper part of the Zaonega Formation. The outcrop displays layers of organic-rich mudstones, dolostones and thin seams of lustruous pyrobitumen. Both the

mudstones and overlying cherts contain numerous large carbonate concretions (Melezhik et al., 1999). Many of these mudstones and dolostones contain elevated concentrations of phosphate, mostly in the form of fluorapatite, which occur in impure layers, lenses and nodules (Lepland et al., submitted).

Figure 2: Panorama of the Shunga village outcrop. Red dot indicates approximate location of the samples.

Materials and methods

Samples were taken from Zaonega Formation organic rich mudstones and dolostones in Shunga village outcrop (62° 35' 32,11" N 34° 55' 38,46" E). From three profiles a total of 47 samples were collected. The stratigraphic position of the samples used in this study are indicated on figure 3.
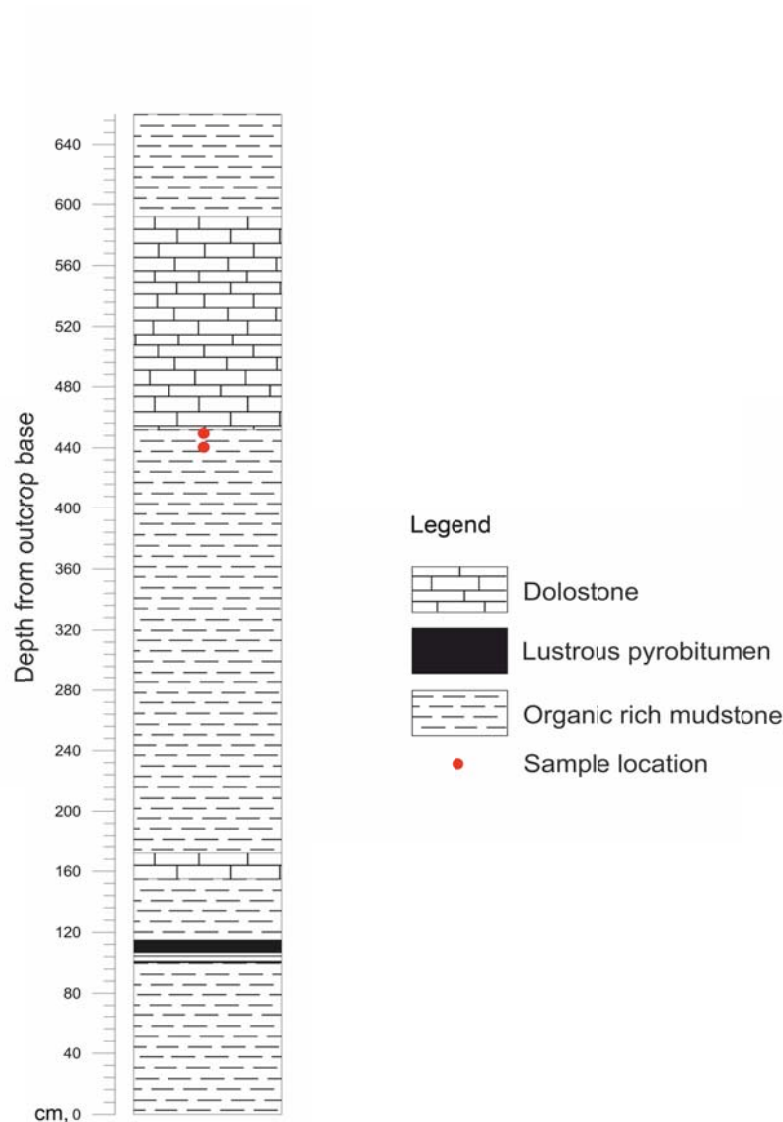

Figure 3: Lithographic column of the Shunga outcrop and stratigraphic position of the samples used in this study.

Samples containing an elevated concentration of phosphate were chosen and prepared for scanning electron microscope (SEM) imaging (Figure 4). Polished surfaces perpendicular to bedding were mostly encased in epoxy, though some samples were inspected as broken surfaces. Freshly broken surfaces, made perpendicular to bedding, were imaged both with a coating of 5 nm thick Pt conductive layer (using Leica EM SCD 500 high-resolution sputter)

and without. The images used in this study were captured in back-scattered electron (BSE) mode on a ZEISS EVO MA15 SEM at Tartu University. In cases where uncoated samples started charging, variable pressure mode of the SEM was used.

Figure 4: A polished surface of a sample from Shunga village outcrop organic-rich mudstone. Abundant dark phosphatic layers and nodules are visible. The length of the sample is approximately 4 cm.

From captured images and directly under SEM the sizes of phosphatic nodules and cylindrical apatite particles were measured. In flattened phosphatic nodules the shortest and longest diameters were measured. Altogether 323 phosphatic nodule cross-sections were acquired. Ellipsoidal cross-sections of nodules were corrected into circular shapes, assuming that the area of a cross-section did not change during compaction. However, it must be considered that the diameters on these 2-dimensional cross-sections do not represent a true diameter of the 3-dimensional objects (e.g. Nauman and Cavanaugh, 1998). Therefore, it was necessary to correct the measurements, using the formula provided by Stoyan (1990), for which it was assumed that the particles were spherical and did not intersect with each other. The observed system can be considered as a polydispersal system with particles which have the same shape but different size (Sahagian and Proussevitch, 1998).

The dimensions of apatitic micrometer-size cylinders were measured under SEM at high magnification >10,000 times. To avoid distortion of true lengths and diameters, only those cylinders, whose long axis was parallel to the plane of the cross-section, were used in the case of length measurements. When measuring diameters, cylinders whose long axes were perpendicular to the plane were used. Altogether, 120 length measurements and 125 diameter measurements were made.

For microstructural studies Focused Ion Beam (FIB) sample preparation of selected apatitic cylinders was carried out via FEI FIB2000-TEM at GeoForschungsZentrum Potsdam. Under FIB ultrathin (100 nm) slabs transparent to the electron beam were cut and the samples were then examined with a FEI TecnaiG2 F20 X-TWIN transmission electron microscope (TEM), also at GeoForschungsZentrum Potsdam. The TEM imaging and analysis was done using a Fishione high-angle annular dark-field detector (HAADF), Gatan Imaging Filter (GIF) and EDAX X-ray analyzer.

Results and discussion

Nodular apatite

Apatite occurs in a 15 cm interval beneath the dolostone layer, in the upper part of the exposed section of organic-rich mudstone in the Shunga village outcrop. Scanning electron microscopy of polished surfaces revealed that phosphate in the samples is contained in a mudstone matrix rich in phlogopite and carbonaceous matter. The phosphate appears either as single (Figure 5a) or clustered (Figure 5b) round-oval nodules of a hundred to several hundred microns in diameter, that are often flattened (Figure 5c) and agglomerated into layers (Figure 5d). Sometimes, the phosphate occurs simply as lamellas surrounding or between the nodules (Figure 5a). Deformation and different degrees of flattening indicate that the nodules were soft during burial. Additionally, some nodules are surrounded by deflected laminae of organic-rich mudstone, which demonstrate further the early, pre-lithification formation of the phosphatic nodules. Lepland et al. (submitted) interpreted these nodules as fossilized casts of microorganisms similar to giant sulfur oxidizing bacteria *Thiomargarita namibiensis*, that are thriving off the coast of Namibia, a site of modern phosphorite precipitation (Schulz, 1999, 2005).

Apatite cylinders

When examined at a higher magnification, the phosphatic nodules and laminae appear to be composed mainly of a multitude of apatitic cylinders of a few microns in length hosted within carbonaceous matter (Figure 5f, 6a). Occasionally, apatite also appears as spherical aggregates with diameters of ca 5 μm (Figure 6f) or as rather homogenous mixtures of apatite and carbonaceous matter, formed when the apatitic particles are pressed together. In several cases, the cylinders seem to be smaller in the vicinity of the nodules' edges, while staying relatively consistent in size within the interiors. SEM and TEM imaging of samples with freshly broken surfaces reveals that several of these cylinders appear to be covered with a c. 30 nm thick film of well-ordered graphitized carbonaceous matter (Figure 6e). These are interpreted to form as a result of mineral-template induced graphitization of carbonaceous matter (van Zuilen et al., 2012).
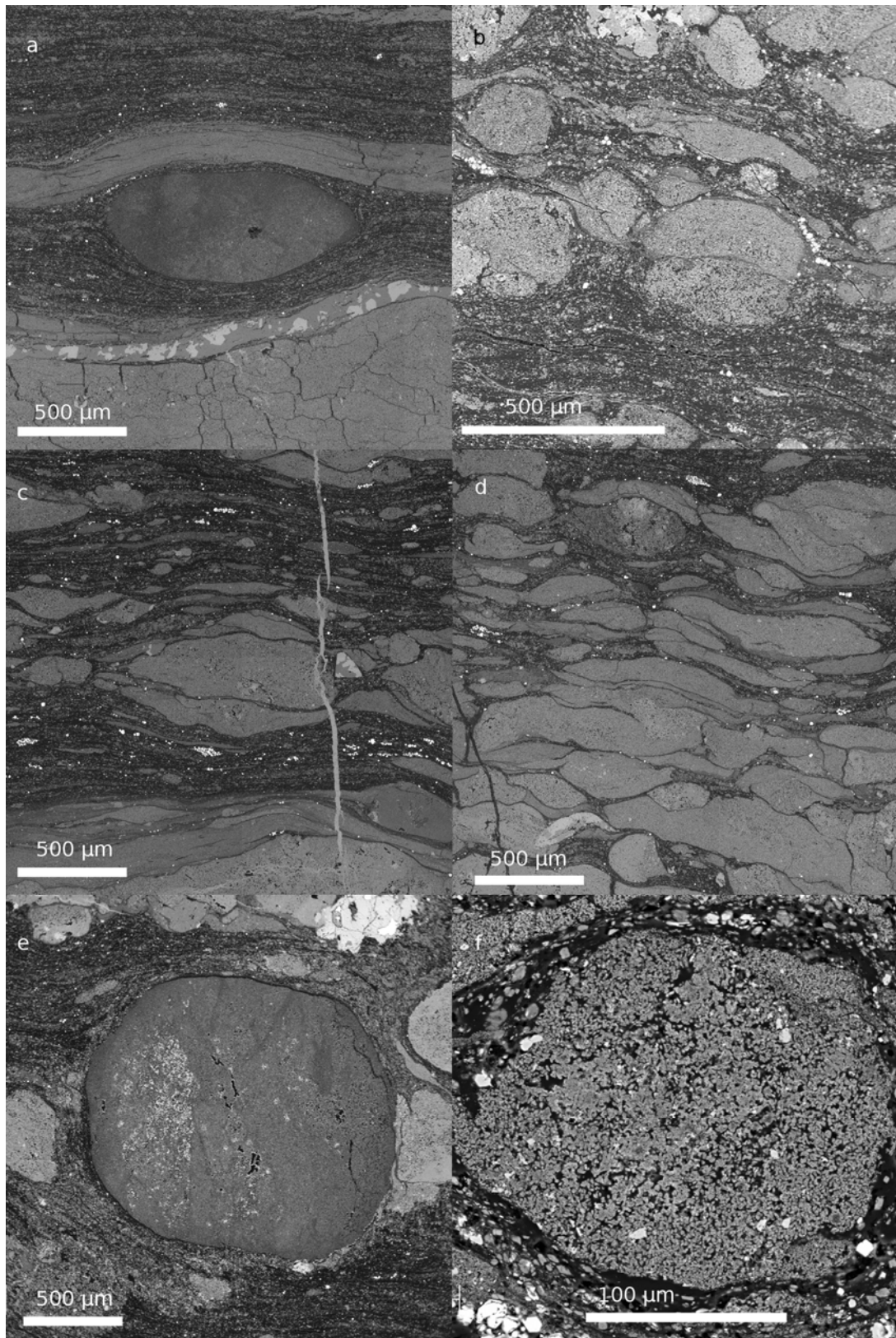
Figure 5: SEM-BSE (scanning electron microscope backscattered electron detector) micrographs of Shunga village outcrop acquired from polished surfaces. Phosphatic layers, lenses and nodules appear lighter than the carbonaceous mudstone, due to a stronger backscatter response of apatite when compared to carbon. **a)** A single relatively unflattened nodule surrounded by phosphatic lamellas. **b)** A cluster of relatively unflattened phosphatic nodules. **c), d)** Flattened phosphatic nodules and lenses. **e)** Fine lamination in mudstones deflects around an unusually large phosphatic nodule. **f)** A close up of a smaller nodule, displaying numerous cylindrical apatitic particles.
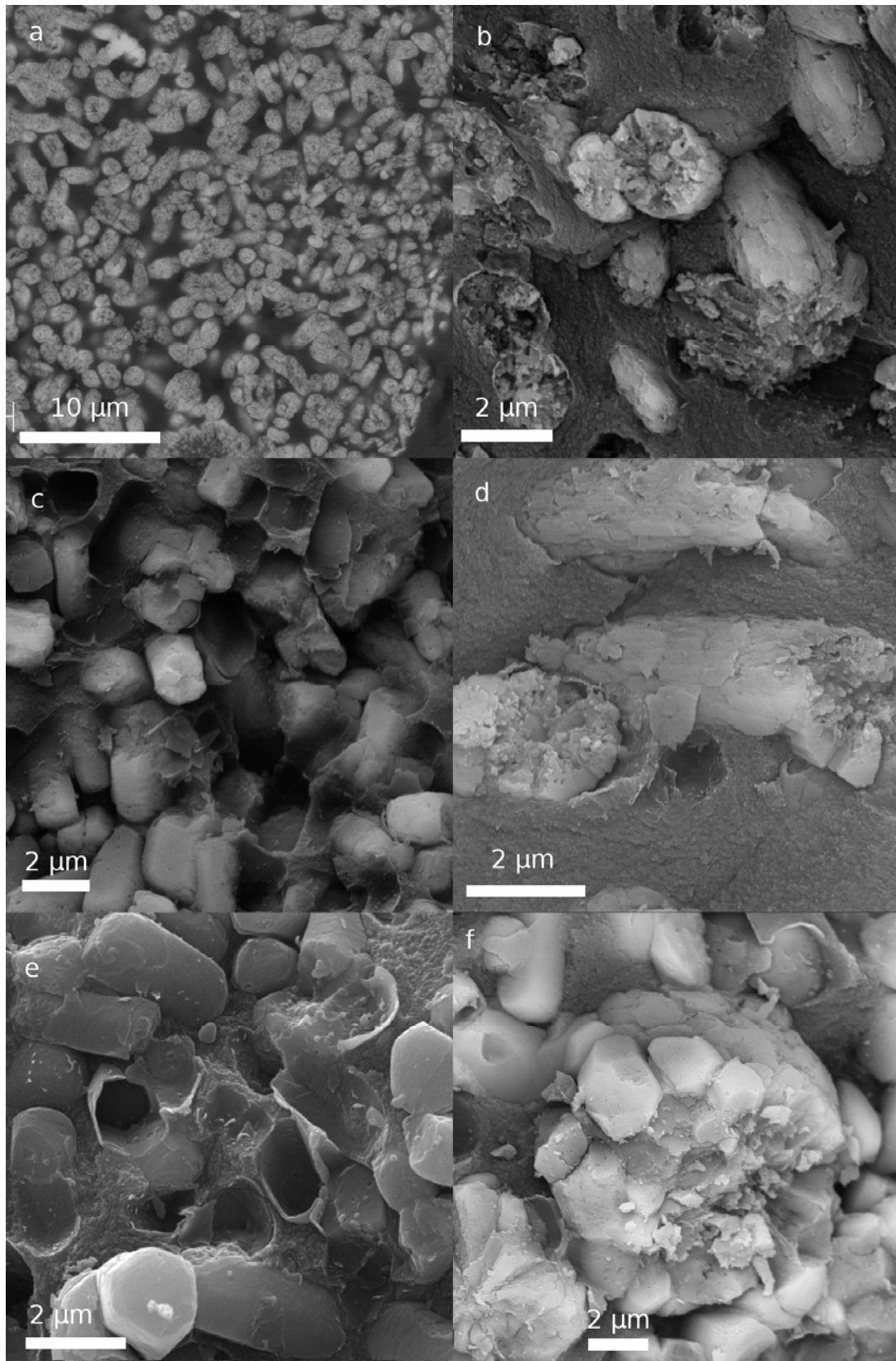
13

Figure 6: SEM-BSE and SE (secondary electron detector) micrographs of apatitic cylindrical particles. **a)** Overview of apatitic cylinders on a polished surface sample, illustrating their abundance. Images b) through f) are obtained from broken surface samples **b)** Relatively well preserved apatitic cylinders displaying an ordered rim, but an unordered interior. **c)** Recrystallized cylinders retaining almost none of their primary inner structure. **d)** Apatite crystallites on the surface of a cylinder resembling a fish-scale structure. **e)** Graphitized films that surrounded poorly preserved cylinders prior to the cracking of the sample. **f)** A spherical nodule of apatite.

The internal structure of these particles is highly variable, which is attributed to differing states of preservation of original cylindrical apatitic particles. Different samples and in some cases different nodules within the same sample host cylinders of different preservation states, but preservation state within a single nodule is mostly uniform.

TEM and SEM imaging revealed that the most primary, least re-crystallized particles seem to be surrounded by an ordered sheath of 100-300 nm apatitic crystallites (sometimes in two layers). When the best-preserved cylinders are viewed from the side, the crystallites give them a fish-scale-like appearance (Figure 6d). The inner parts of the cylindrical particles show an unordered mixture of anhedral, inclusion-rich Ca-phosphatic crystallites and carbonaceous matter (Figure 6b, Figure 7). This type of preservation is rare and a great majority of the particles are more-or-less recrystallized, showing radial, if any inner structure, but have maintained the overall size and proportions of the primary particles (Figure 6c).
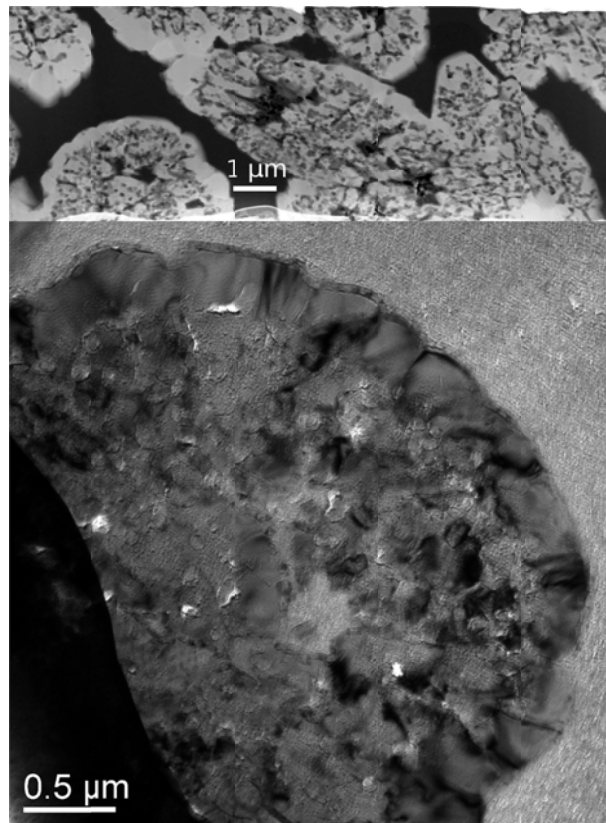

Figure 7: TEM (transmission electron microscope) micrographs of an ultrathin slab cut by focused ion beam milling from the interior of a phosphatic nodule. **a)** High-angle annular dark-field (HAADF) detector image of apatite (bright) cylinders in the matrix of carbonaceous matter (dark). The internal parts of the cylinders are of heterogeneous composition, while the surrounding rim is rather homogenous. **b)** BF (Bright Field) image of a single apatitic cylinder. The outer rim of crystallites is composed of distinctly well-ordered apatite, while the insides show a mix of carbonaceous matter and inclusion-rich anhedral apatite crystals. A thin graphitic film surrounds the cylinder and the crystallites.

15

Size distribution of nodular and cylindrical particles

Though the majority of the phosphatic nodules in the Shunga village samples were broken or flattened to the point of appearing lense-like, those shapes can be interpreted as a degradational collapse and flattening of originally spherical cells during compaction of host organic-rich mudstone. Thus, the size measurements included only more spherical nodules which were thought to have maintained their shape and volume best. These relatively well-preserved nodules, presumably of more or less spherical origin, have nevertheless flattened during burial and diagenesis (Figure 5ab). However, the compaction ratio of nodules is quite similar in different samples and for different sizes. The average ratio of the shortest and longest diameter was 0.67 (Figure 8). The diameters, as measured from the polished surfaces and then corrected for circular shape, are shown in figure 9a. The mean of apparent diameters uncorrected for 3D distribution was 385 μm. The systematical underrepresentation of smaller nodules results, however, in the shift of the mean towards higher values. After correction, the mean of the nodules distribution was estimated at 336 μm (Figure 9b), while the values of the diameters ranged from 60 μm to an exceptional maximum of 2700 μm. Still, diameters of over 600 μm occurred only in 5% of the measured and corrected nodules.

Microorganisms of similar size and shape are the giant sulfur oxidizing bacteria *Thiomargarita namibiensis* that are important drivers of phosphogenesis in modern shelf environment, off the coast of Namibia (Schulz, 1999, 2005). The reported diameters of *Thiomargarita namibiensis* specimens are mainly in the range of 100-300 μm, while some few reach over 750 μm (Schulz, 1999). Though the studied material contains large phosphatic nodules that exceed over 2 times the known sizes of *Thiomargarita* cells, the average size of these nodules agrees well with the reported ranges for large sulfur-bacteria and only few percent of the corrected measurements lie outside reported *Thiomargarita* sizes. Moreover, recently Girnth et al. (2011) reported a mat-forming population of the giant sulfur bacteria *Thiomargarita* at the flank of the mud volcano Amon on the Nile Deep Sea Fan in the Eastern Mediterranean Sea, where *Thiomargarita* cells are with a diameter of 24-65 μm, substantially smaller than cells of previously described populations. This discovery shows that the size of *Thiomargarita* can be highly variable, and size cannot be used as sole argument for or against *Thiomargarita*-like cells.
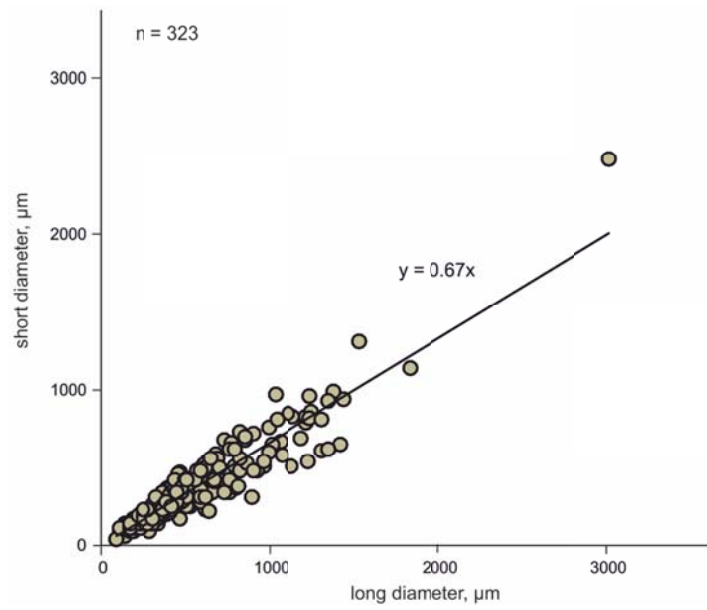
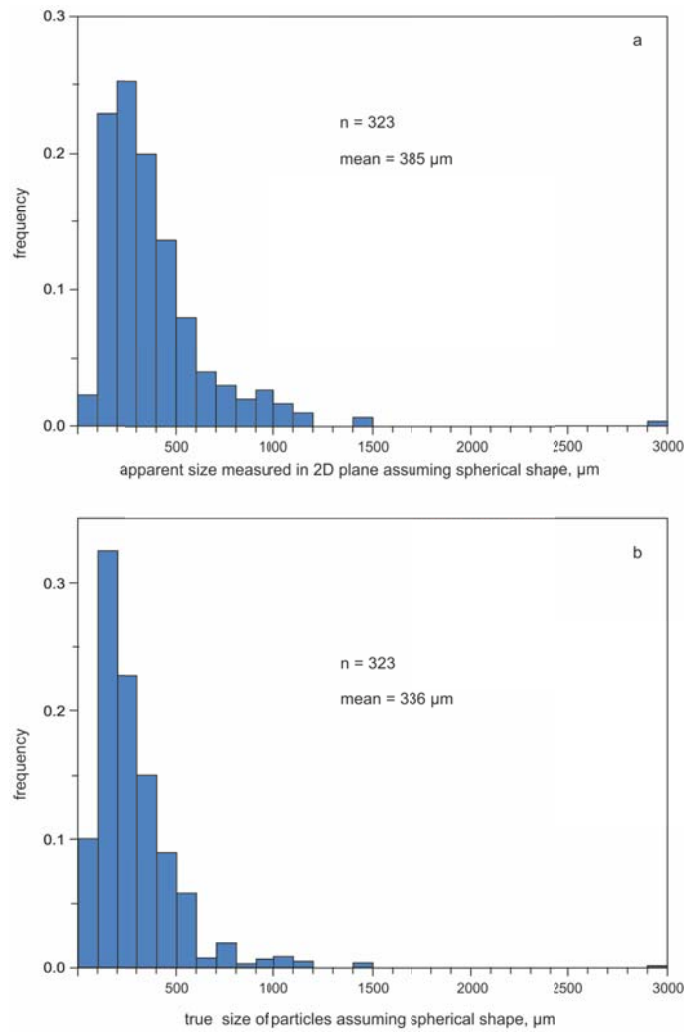Figure 8: Measured long and short diameters of phosphatic nodules.

Figure 9: **a)** Apparent diameters of nodules in a 2D-plane, when corrected for spherical shape, assuming the area of the section did not change during compaction. **b)** True calculated diameters of nodules assuming that the nodules are spherical and do not intersect.
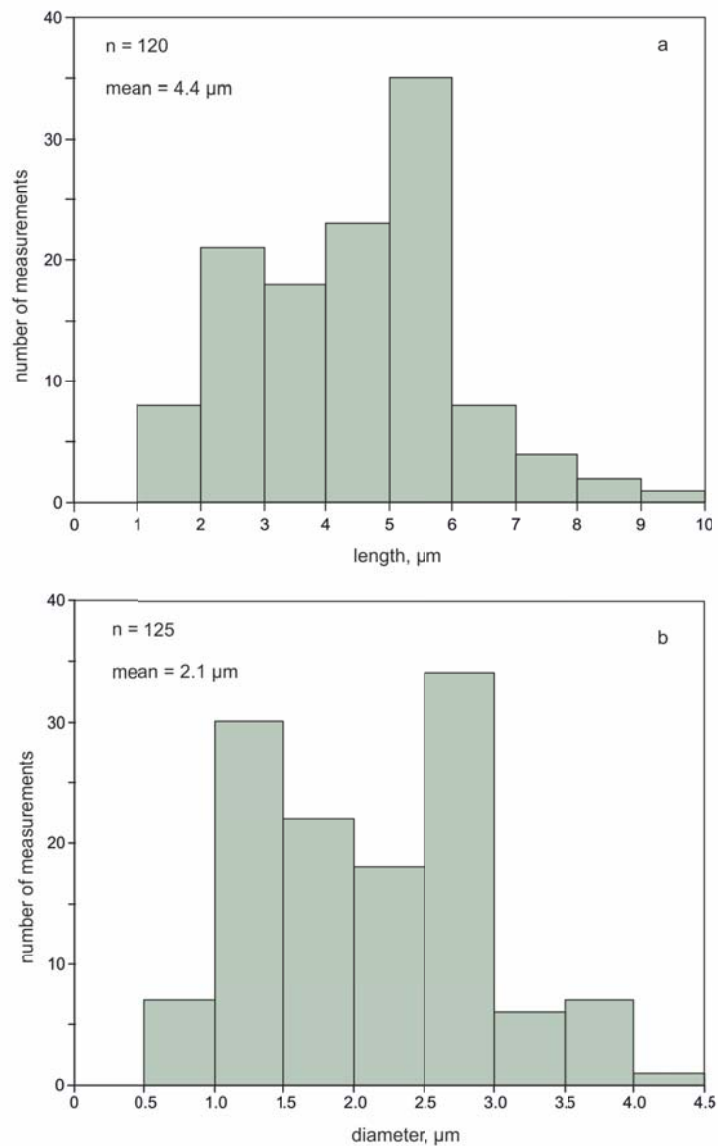
Figure 10: Apparent **a)** lengths and **b)** diameters of the measured apatitic particles.

The apparent lengths and diameters of cylindrical apatitic particles contained within and around the larger phosphatic nodules are shown in figure 10. The lengths of the measured particles ranged from c. 1 to 8 μm (mean 4.4 μm, standard deviation of 1.6 μm) and diameters from c. 0.5 to 4 μm (mean 2.1, standard deviation 0.8 μm).

In comparison, modern methanotrophic archea ANME-1 found in cold methane seeps in the Black Sea have lengths of 1.5-3 μm and diameters of about 0.6 μm (Knittel et al., 2005). Though some apatitic cylinders appear over two times larger than ANME-1, their lower size range agrees well with modern ANME-1 sizes.

Structure types, different preservation states of apatitic cylinders

The preservation states of the apatitic cylinders form a continuum between the best-preserved particles, which host the finest apatitic crystallites on their surfaces and those that are completely recrystallized. Here, I have subdivided the preservation states into four general categories from best to least preserved.

1. The best-preserved particles are surrounded by numerous distinct and well-ordered apatite crystallites of a few hundred nanometers in length, which are perpendicular to the outer surface. When a particle is viewed from the side, the crystallites form a structure resembling fish-scales. The interior of the particles is however composed of an unordered mixture of inclusion-rich anhedral Ca-phosphatic crystallites and carbonaceous matter. The cross-section of the particles is smooth and circular (Figure 11a).

2. Similar to above, but the encircling crystallites have started to coalesce and grow inwards. The outer shape of the cylinder can be smooth or slightly hexagonal (Figure 11b).

3. The crystallites have coalesced further and fill most of the interior of the particle, forming a radial shape. Phosphatic-carbonaceous matter is present in the very center as a thin, protruding rod-like structure. The outer shape of the particle is likely to be hexagonal, but not always (Figure 11c).

4. Completely recrystallized particles, which still maintain similar sizes and proportions to the primary cylinders, but show hexagonal crystal habit. None of the central unordered phosphatic-carbonaceous material is present, having been replaced by inclusion-rich apatite (Figure 11d).

These categories are only generalizations based on the most common consortia of traits. Traits from wholly different categories can still coexist in cases of rarer particles.

Formation mechanism of cylindrical particles and nodules

Cylindrical apatite particles of few micrometers in size are not uncommon and have mostly been interpreted as compact particles formed as a result of rapid nucleation events in pore-water medium (Krajewski et al., 1994; Baturin, 2002; Baturin and Titov, 2006). However, similar particles have been considered as intracellularly phosphate-replaced bacterial cells (e.g.

19

Soudry and Lewy, 1988; Lamboy 1990, 1994; Rao and Lamboy, 1996; Rao et al., 2000, Sanchez-Navas and Martin-Algarra, 2001).
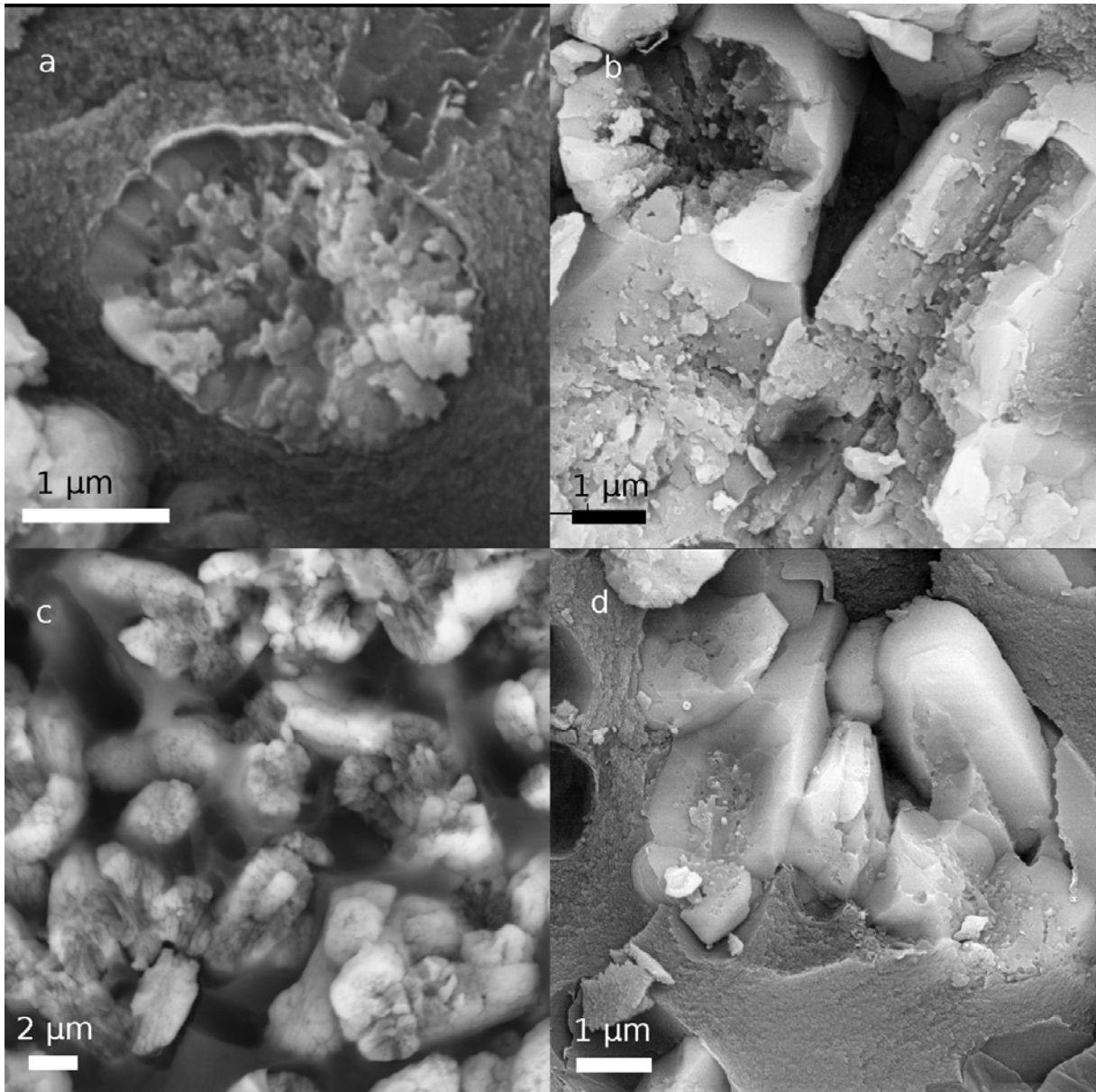

Figure 11: SEM-BSE micrographs of different states of preservation of cylindrical apatitic particles in broken surface samples. a) A rim of uniform well-ordered apatite crystals surrounds a well-preserved cylinder. b) Cylinders in a slightly lower state of preservation rimmed by apatite crystallites, which show signs of inward growth. c) Cylinders displaying a protruding rod of unordered material surrounded by radially occurring apatite crystallites. d) Hexagonal, completely recrystallized cylinders. Note the abundant inclusions in the interior of the cylinder.

Apatitic cylinders in Zaonega Formation organic-rich mudstones can be interpreted as phosphatic replacement structures similar in shape, size and petrographic distribution to modern methanotrophic archea ANME-1 and ANME-2, which inhabit modern microbial mats in deep-sea methane seep localities and often form close associations with sulfur-oxidizing

microbes that use hydrogen sulfide formed as by-product of anaerobic oxidation of methane as an energy source (Knittel et al., 2005).

The consistent sizes and shapes of these apatitic particles throughout the several samples, similar to cylinder and rod-shaped apatite particles reported in other phosphorites (e.g. Krajewski et al. 1994), are not characteristic of inorganically precipitated apatite, which would produce particles of variable shapes and sizes according to changes in chemical environment of the pore water.

Similarity to ANME-1 populations is evident in the shapes, sizes and distribution of the particles. Apatitic particles in the Zaonega Formation samples appear as very dense collections of individual and rarely clustered rod-shaped structures with diameters and lengths of a few micrometers. Modern ANME-1 populations in microbial mats on the Black Sea floor are also extremely dense (Knittel et al., 2005). A cubic centimeter of Black Sea microbial mat could contain up to $9*10^{10}$ cells, and ANME-1 represented up to 50% or 70% of the total number. The cylindrical (or rarely clustered) cells have lengths of a few micrometers, diameters of less than a micrometer and a biovolume of about 1 μm^3, which taken together means that ANME-1 dominate the microscale appearance of the microbial mats (Michaelis et al., 2002; Knittel et al., 2005), a situation very similar to that observed in the Zaonega samples with cylindrical apatite particles (Michaelis et al., 2002; Knittel et al., 2005).

The outer shell of cylindrical, rod shaped particles is composed of apatite particles perpendicularly arranged to the outer surface, which we interpret as apatite crystallites formed from amorphous precursors and mediated by solid phase mineralization on the bacterial cell membranes. In membranes the functional groups in the organic matrix are periodically arranged, and thus promote heterogeneous nucleation of crystalline phases. This likely occurred while the cells were still metabolically active.

Some of the fossilized rod shape microorganisms show a double layering of the exterior shell, which we interpret as fossilized remains of layered membrane structures. As the putative methanotrophs died and decayed, we propose that the nanometer size crystallites in the apatitic rim started to merge-recrystallize and grow inward in the diagenetic environment due to thermodynamic forcing, replacing the anhedral Ca-phosphate and organic phases until the former cells consisted of a single inclusion-rich apatite crystal with a hexagonal outer appearance (Figure 12).
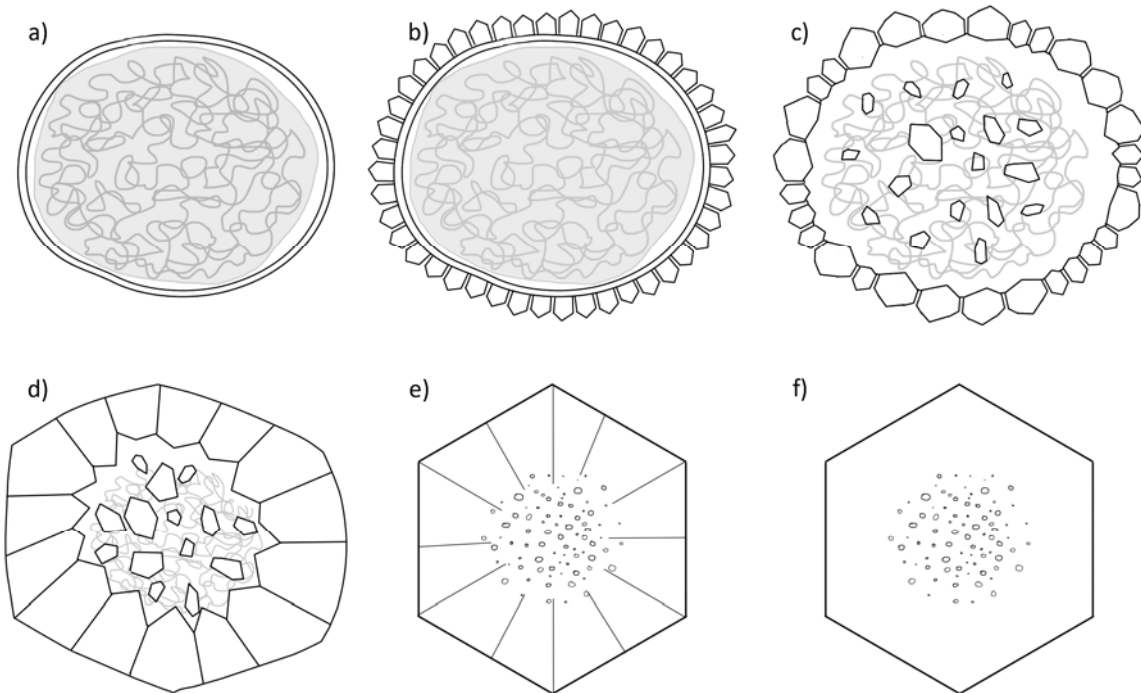
Figure 12: A schematic representation of the mineralization process of putative methanotrophic archea fossils from primary state to most altered. a) Cross-section of an actively metabolizing archeal cell, showing intact cell membrane and cytoplasm. b) Heterogenous nucleation of apatite on the cell membrane has produced a rim of ordered crystallites surrounding the still metabolizing archea. c) The archea has perished, and the cell membrane and cytoplasm have decayed. The ordered apatite crystallites on the rim have started to coalesce and grow inward, while the center of the fossil is filled with an unordered mix of anhedral, inclusion-rich Ca-phosphate crystals and carbonaceous matter. d) The ordered apatitic crystallites on the rim have grown and coalesced further. A radial structure is starting to develop around a central rod of unordered Ca-phosphatic crystals and carbonaceous material. The fossil is starting to obtain a hexagonal shape. e) The outer shape of the fossil has become more or less hexagonal, while the cross-section shows a distinct radial structure, formed by the growing crystals, which now encompass almost the entirety of the fossil. f) The fossil has completely recrystallized into a single hexagonal apatitic crystal, which has a distinctly inclusion-rich center.

We interpret the phosphatic nodules in Zaonega Formation samples to be casts of giant sulfide-oxidizing bacteria similar to modern *Thiomargarita Namibiensis*, which inhabit marine sediments off the coast of Namibia and are known to mediate the formation of phosphorites via the hydrolyzation of stored polyphosphate and release of phosphate into sediment pore water in sulfidic conditions, which can then precipitate as apatite, using microbial cell walls as templates (Schulz and Schulz, 2005).

The nodules present in Zaonega Formation mudstones seem to be morphologically consistent with recent work on the taphonomy of *Thiomargarita* cells. In Shunga village samples, the nodules are present mainly in chains and show different levels of flattening and distortion. While the outer shape of the nodules is usually distinct, the interior is devoid of large-scale

22

structure and is composed of a homogenous mass of cylindrical apatite particles and carbonaceous matter. In a recent taphonomic study by Cunningham et al. (2012), the most labile parts of *Thiomargarita* cells were found to be its interior structures – the vesicles, giant central vacuole and surrounding cytoplasm. As these degraded, the interior spaces of the cells were filled with a diffuse amorphous organic matter with no visible structure, while the surrounding laminar sheets and mucous sheath showed no signs of degradation. Eventually the laminar sheets disintegrated, leaving the mucous sheath as the most resilient, taking as long as months or years to degrade. During this period, the cells started to distort and the mucous sheaths often combined to form chains of differently preserved cells. There is a considerable temporal window available for the mineralization of *Thiomargarita*-like bacteria, due to the long perseverance of the mucous sheath. In light of the high mineralization potential of the exopolymeric substances present in the mucous sheath (Pacton et al., 2007), Cunningham et al. (2012) concludes that the likelihood of finding *Thiomargarita*-like fossils in ancient microbial mats with an intact outer shape but a homogenized inner structure is high.

It can be proposed that as the putative sulfur bacteria in the ancient Onega basin died and decayed, some collapsed or disintegrated, while others were preserved as relatively spherical nodules, if the surrounding sediment was previously somewhat solidified with the phosphate secreted by the sulfur bacteria themselves. The cavities left after decomposition of the bacteria interiors were colonized by methane-metabolizing archea, whose membranes proved to be templates for heterogenous nucleation of apatite. This caused the eventual phosphatization of the archea and further aided in preventing the collapse of the nodular cell walls. This sequence of microbial activity, in which methanotrophic archea post-date the sulfur-oxidizers is consistent with diagenetic sequence of thermodynamically determined oxidant depletion (e.g. Froelich et al., 1979). Oxygen and nitrate as used by sulfide-reducing bacteria are depleted earlier than sulfate, which is used by anaerobic methanotrophs.

Summary and conclusions

The phosphatic nodules and apatitic particles present in Zaonega Formation organic-rich mudstones have intriguing morphologies reminiscent of modern day microbial communities. The possible biological chemistry of these putative fossils is however lost, as can be expected due to its low preservation potential, especially when organic structures are replaced or mineralized. Thus, morphological criteria and the syngenetic environment are left for testing the biogenicity of these structures.

The large phosphatic nodules, have been interpreted as casts of ancient bacteria similar to modern large sulfur-metabolizing *Thiomargarita namibiensis,* which occurs in phosphatic sea sediments off the coast of Namibia. The Zaonega Formation nodules are roughly spherical or flattened, occasionally appearing in isolation, but more often agglomerated into chains or layers. The nodules diameters show a nearly normal distribution and range from 100 to 2700 μm with a mean of 336 μm, which is consistent, if slightly larger with the size distribution reported for modern spherical *Thiomargarita* cells, which can be up to 750 μm in diameter. The size discrepancy is however not large, as only a few percent of measured Zaonega Formation nodules are bigger than modern *Thiomargarita* cells. The putative *Thiomargarita* fossils show no inner cellular structure, but consist rather of a homogenous mass of cylindrical apatitic particles, which are interpreted to represent a fossilized microbial community, which colonized the cellular cavity of the putative cell after its cytoplasma decayed. This along with the shapes of the nodules agrees with taphonomical studies of *Thiomargarita* populations, where it was found that the interior of the cells decayed relatively quickly into a homogenous mass, while the mucous sheath remained intact for months, deforming into various shapes. Additionally, *Thiomargarita* are known to mediate the precipitation apatite via the release of phosphate into pore water as part of an auxiliary metabolic process, which would explain the abundant apatite found within studied Zaonega Formation samples.

The cylindrical apatite particles, of which the phosphate in Zaonega Formation samples is composed, have been interpreted as mineralized methanotrophic archea similar to modern ANME-1 clades found in Black Sea methane seep sites. The cylinders show very consistent shapes and sizes uncharacteristic of inorganically formed apatite particles, which would display a range of morphologies and sizes according to changes in the surrounding chemical environment. The lengths (1 to 8 μm) and diameters (0.5 to 4 μm), are only slightly larger

than the 1-3 μm reported in modern ANME-1. The abundance and concentration of putative fossils within the mudstone also agree with the dense populations reported for ANME-1. The best-preserved cylinders show inner structure consistent with nucleation of apatite on cell membranes, a well-established process of microbial biomineralization. Several states of preservation can be observed, from cylinders with an ordered outer shell of apatite to those that are completely recrystallized.

The interpreted consortium of methanotrophs and sulfur-oxidizing bacteria in Zaonega formation is analogous to those found in modern methane-seep sites, where sulfur-oxidizing bacteria form consortia with ANME-1 methanotrophs.

Acknowledgments

References

Arning, E T, Birgel, D., Brunner, B., & Peckmann, J. (2009). Bacterial formation of phosphatic laminites off Peru. Geobiology, 7(3), 295–307. doi:10.1111/j.1472-4669.2009.00197.x

Arning, Esther T., Birgel, D., Schulz-Vogt, H. N., Holmkvist, L., Jorgensen, B. B., Larson, A., & Peckmann, J. (2008). Lipid Biomarker Patterns of Phosphogenic Sediments from Upwelling Regions. Geomicrobiology Journal, 25(2), 69–82. doi:10.1080/01490450801934854

Bailey, J. V, Joye, S. B., Kalanetra, K. M., Flood, B. E., & Corsetti, F. a. (2007). Evidence of giant sulphur bacteria in Neoproterozoic phosphorites. Nature, 445(7124), 198–201. doi:10.1038/nature05457

Baturin, G. N. (2002). Nodular Fraction of Phosphatic Sand from the Namibia Shelf. Lithology and Mineral Resources, 37(1), 1–17. doi:10.1023/A:1013628020381

Bekker, A., Holland, H. D., Wang, P.-L., Rumble, D., Stein, H. J., Hannah, J. L., Coetzee, L. L., et al. (2004). Dating the rise of atmospheric oxygen. Nature, 427(6970), 117–20. doi:10.1038/nature02260

Buick, R. (1990). Microfossil recognition in Archean rocks: an appraisal of spheroids and filaments from a 3500 my old chert-barite unit at North Pole, Western Australia. Palaios, 5(5), 441–459.

Buseck, P., Galdobina, L., Kovalevski, V., Rozhkova, N., Valley, J., & Zaidenberg, A. (1997). Shungites; the C-rich rocks of Karelia, Russia. The Canadian Mineralogist, 35, 1363–1378.

Butterfield, N. (2003). Exceptional fossil preservation and the Cambrian explosion. Integrative and Comparative Biology, 43(1), 166–177. doi:10.1093/icb/43.1.166

Cohen, P. A., Schopf, J. W., Butterfield, N. J., Kudryavtsev, A. B., & Macdonald, F. A. (2011). Phosphate biomineralization in mid-Neoproterozoic protists. Geology, 39(6), 539–542. doi:10.1130/G31833.1

Crne, A. E., Melezhik, V. A., Prave, A. R., Lepland, A., Romashkin, A. E., Rychanchik, D. V., Hanski, E. J., et al. (2013). 6.3.3 Zaonega Formation: Zaonega Formation: FAR-DEEP Holes 12A and 12B, and neighbouring quarries. In V. A. Melezhik, A. R. Prave, A. E. Fallick, E.

Hanski, A. Lepland, L. R. Kump, & H. , Strauss (Eds.), Reading the Archive of Earth's Oxygenation, vol. II (pp. 946–1007). Springer. doi:10.1007/978-3-642-29659-8_4

Cunningham, J. a, Thomas, C.-W., Bengtson, S., Marone, F., Stampanoni, M., Turner, F. R., Bailey, J. V, et al. (2012). Experimental taphonomy of giant sulphur bacteria: implications for the interpretation of the embryo-like Ediacaran Doushantuo fossils. Proceedings. Biological sciences / The Royal Society, 279(1734), 1857–64. doi:10.1098/rspb.2011.2064

Ellison, S. (1944). The composition of conodonts. Journal of Paleontology, 18(2), 133–140. doi:10.2307/1299017

Filippelli, G. (2011). Phosphate rock formation and marine phosphorus geochemistry: the deep time perspective. Chemosphere, 84(6), 759–766. doi:10.1016/j.chemosphere.2011.02.019

Föllmi, K. B. (1996). The phosphorus cycle, phosphogenesis and marine phosphate-rich deposits. Earth-Science Reviews, 40(1–2), 55–124. doi:10.1016/0012-8252(95)00049-6

Goldhammer, T., Brüchert, V., Ferdelman, T. G., & Zabel, M. (2010). Microbial sequestration of phosphorus in anoxic upwelling sediments. Nature Geoscience, 3(8), 557–561. doi:10.1038/ngeo913

Knittel, K., Lösekann, T., Boetius, A., Kort, R., & Amann, R. (2005). Diversity and distribution of methanotrophic archaea at cold seeps. Applied and environmental microbiology, 71(1), 467–79. doi:10.1128/AEM.71.1.467-479.2005

Krajewski, K. P., Van Capellen, P., Trichet, J., Kuhn, O., Lucas, J., Martin-Algarra, A., Prevot, L., et al. (1994). Biological Processes and Apatite Formation in Sedimentary Environments. Eclogae Geologicae Helvetiae, 87(3), 701–745.

Lamboy, M. (1990). Microbial mediation in phosphatogenesis: new data from the Cretaceous phosphatic chalks of northern France. Geological Society, London, Special Publications, 52(1), 157–167. doi:10.1144/GSL.SP.1990.052.01.11

Lamboy, Michel, Rao, V. P., Ahmed, E., & Azzouzi, N. (1994). Nanostructure and significance of fish coprolites in phosphorites. Marine Geology, 120(3-4), 373–383. doi:10.1016/0025-3227(94)90068-X

Lepland, A, Melezhik, V. A., Papineau, D., Romashkin, A. E., & Joosu, L. (2013). The earliest phosphorites: Radical change in the phosphorus cycle during the palaeoproterozoic. Frontiers in Earth Sciences (Vol. 8, pp. 1275–1296). doi:10.1007/978-3-642-29670-3_7

Lepland, Aivo, Joosu, L., Kirsimäe, K., Prave, A. R., Romashkin, A. E., Črne, A. E., Martin, A., et al. (submitted). Fossilisation by phosphatisation 2 billion years ago. Manuscript. Nature Geoscience.

Melezhik, V. A., Fallick, A. E., Filippov, M. M., & Larsen, O. (1999). Karelian shungite—an indication of 2.0-Ga-old metamorphosed oil-shale and generation of petroleum: geology, lithology and geochemistry. Earth-Science Reviews, 47(1-2), 1–40. doi:10.1016/S0012-8252(99)00027-6

Melezhik, V. A., Filippov, M. M., & Romashkin, A. E. (2004). A giant Palaeoproterozoic deposit of shungite in NW Russia: genesis and practical applications. Ore Geology Reviews, 24(1-2), 135–154. doi:10.1016/j.oregeorev.2003.08.003

Michaelis, W., Seifert, R., Nauhaus, K., Treude, T., Thiel, V., Blumenberg, M., Knittel, K., et al. (2002). Microbial reefs in the Black Sea fueled by anaerobic oxidation of methane. Science (New York, N.Y.), 297(5583), 1013–5. doi:10.1126/science.1072502

Nauman, E. B., & Cavanaugh, T. J. (2005). Method of Calculating True Particle Size Distributions from Observed Sizes in a Thin Section. Microscopy and Microanalysis, 4(02), 122–127. doi:10.1017/S1431927698980102

Nelson, G., Pufahl, P., & Hiatt, E. (2010). Paleoceanographic constraints on Precambrian phosphorite accumulation, Baraga Group, Michigan, USA. Sedimentary Geology, 226(1–4), 9–21. doi:10.1016/j.sedgeo.2010.02.001

Ojakangas, R. W., Marmo, J. S., & Heiskanen, K. I. (2001). Basin evolution of the Paleoproterozoic Karelian Supergroup of the Fennoscandian (Baltic) Shield. Sedimentary Geology, 141-142, 255–285. doi:10.1016/S0037-0738(01)00079-3

Pacton, M., Fiet, N., & Gorin, G. E. (2007). Bacterial Activity and Preservation of Sedimentary Organic Matter: The Role of Exopolymeric Substances. Geomicrobiology Journal, 24(7-8), 571–581. doi:10.1080/01490450701672042

Papineau, D. (2010). Global biogeochemical changes at both ends of the Proterozoic: insights from phosphorites. Astrobiology, 10(2), 165–181. doi:10.1089/ast.2009.0360

Pufahl, P. K., & Hiatt, E. E. (2012). Oxygenation of the Earth's atmosphere–ocean system: A review of physical and chemical sedimentologic responses. Marine and Petroleum Geology, 32(1), 1–20. doi:10.1016/j.marpetgeo.2011.12.002

Pukhtel, I. S., Zhuravlev, D. Z., Ashikhmina, N. A., & others. (1992). The Sm-Nd Age of the Suisarskaya Formation in the Baltic Shield. Dokl. Akad. Nauk, 326(4), 706–711.

Qu, Y., Crne, A. E., Lepland, A., & Van Zuilen, M. a. (2012). Methanotrophy in a Paleoproterozoic oil field ecosystem, Zaonega Formation, Karelia, Russia. Geobiology, 10(6), 467–78. doi:10.1111/gbi.12007

Rao, V. P., Rao, K. M., & Raju, D. S. N. (2000). Quaternary Phosphorites from the Continental Margin Off Chennai, Southeast India: Analogs of Ancient Phosphate Stromatolites. Journal of Sedimentary Research, 70(5), 1197–1209. doi:10.1306/012400701197

Rao, V.Purnachandra, & Lamboy, M. (1996). Genesis of apatite in the phosphatized limestones of the western continental shelf of India. Marine Geology, 136(1-2), 41–53. doi:10.1016/S0025-3227(96)00062-X

Ruben, J., & Bennett, A. (1987). The evolution of bone. Evolution, 41(6), 1187–1197. doi:10.2307/2409087

Sahagian, D. L., & Proussevitch, A. A. (1998). 3D particle size distributions from 2D observations: stereology for natural applications. Journal of Volcanology and Geothermal Research, 84(3-4), 173–196. doi:10.1016/S0377-0273(98)00043-2

Sánchez-Navas, A., & Martín-Algarra, A. (2001). Genesis of apatite in phosphate stromatolites. European Journal of Mineralogy, 13(2), 361–376. doi:10.1127/0935-1221/01/0013-0361

Schenau, S. ., Slomp, C. ., & De Lange, G. . (2000). Phosphogenesis and active phosphorite formation in sediments from the Arabian Sea oxygen minimum zone. Marine Geology, 169(1-2), 1–20. doi:10.1016/S0025-3227(00)00083-9

Schopf, J. W. (2004). Earth's earliest biosphere: status of the hunt. The Precambrian earth: Tempos and events, 12, 516–591.

Schopf, J. W., Kudryavtsev, A. B., Agresti, D. G., Czaja, A. D., & Wdowiak, T. J. (2005). Raman imagery: a new approach to assess the geochemical maturity and biogenicity of permineralized precambrian fossils. Astrobiology, 5(3), 333–71. doi:10.1089/ast.2005.5.333

Schopf, J. W., Kudryavtsev, A. B., Czaja, A. D., & Tripathi, A. B. (2007). Evidence of Archean life: Stromatolites and microfossils. Precambrian Research, 158(3-4), 141–155. doi:10.1016/j.precamres.2007.04.009

Schopf, J. W., & Walter, M. R. (1983). Archean microfossils- New evidence of ancient microbes. Earth's earliest biosphere: Its origin and evolution(A 84-43051 21-51). Princeton, NJ, Princeton University Press, 1983,, 214–239.

Schulz, Heide N, & Schulz, H. D. (2005). Large sulfur bacteria and the formation of phosphorite. Science (New York, N.Y.), 307(5708), 416–8. doi:10.1126/science.1103096

Schulz, HN N. (1999). Dense Populations of a Giant Sulfur Bacterium in Namibian Shelf Sediments. Science, 284(5413), 493–495. doi:10.1126/science.284.5413.493

Soudry, D., & Lewy, Z. (1988). Microbially influenced formation of phosphate nodules and megafossil moulds (Negev, Southern Israel). Palaeogeography, Palaeoclimatology, Palaeoecology, 64(1-2), 15–34. doi:10.1016/0031-0182(88)90139-3

Stoyan, D. (1990). Stereological formulae for a random system of non-intersecting spheres. Statistics, 21(1), 131–136. doi:10.1080/02331889008802233

Van Zuilen, M. A., Fliegel, D., Wirth, R., Lepland, A., Qu, Y., Schreiber, A., Romashkin, A. E., et al. (2012). Mineral-templated growth of natural graphite films. Geochimica et Cosmochimica Acta, 83, 252–262. doi:10.1016/j.gca.2011.12.030

Williams, A., Mackay, S., & Cusack, M. (1992). Structure of the Organo-Phosphatic Shell of the Brachiopod Discina. Philosophical Transactions: Biological Sciences, 337(1279), 83–104.

Xiao, S., Zhang, Y., & Knoll, A. H. (1998). Three-dimensional preservation of algae and animal embryos in a Neoproterozoic phosphorite. Nature, 391(6667), 553–558. doi:10.1038/35318

Kokkuvõte

Fossiliseerunud väävlibakterite ja metanotroofide morfoloogia ning struktuur 2,0 Ga vanustes Zaonega kihistu orgaanikarikastes savikivimites

Kaarel Mänd

Fosfaatne biomineralisatsioon on laialt levinud nähtus nii iidsetes kui tänapäevastes meresetetes. Kaasaegsetes ookeanides nagu Namiibia šelf kontrollivad fosfaatsete setendite moodustumist mitmed mikroorganismid, millede hulgas on ka perekonda *Thiomargarita* kuuluvad maailma suurimad bakterid. Need, põhiliselt väävlit metaboliseerivad bakterid suudavad hüdrolüüsida ka polüfosfaati, mille tagajärjena vahendavad settelise fosforiidi teket. Metaanirikastes keskkondades leidub väävlibaktereid assotsiatsioonis metanotroofsete arhedega klaadist ANME-1, kes toodavad jääkproduktina väävlibakteritele vajalikku sulfiidi.

Zaonega kihistu kuulub Loode-Venemaal Karjala kraatoni kaguosas asuva Oneega basseini paleoproterosoiliste settekivimite hulka. Kihistu koosneb põhiliselt orgaanilise aine rikastest dolomiitidest ning savikivimitest, mida liigestavad mitmed vulkaanilised kihid. Kogu Oneega basseini setteline kompleks on läbinud rohekildalise moondefaatsiese. Shunga küla lähedalt on avastatud kõrge fosfaadisisaldusega orgaanilise ainese rikkad savikivimid, kus fosfaat on kontsentreerunud noodulitesse ja apatiitsetesse silindrikestesse, mida võib tõlgendada kui fossiliseerunud väävlibaktereid ja nendega sümbiootlilisi metanotroofseid arhesid. Antud töö eesmärk on kirjeldada Zaonega kihistu kivimites leiduvate Ca-fosfaatsete noodulite ja apatiitsete silindrite morfoloogiat, suurusi ja määrata nende võimalik biogeensus ja fossiliseerumismehhanism.

Shunga küla paljandist pärinevaid lihvitud ja murtud pinnaga proove uuriti mikroskaalal skanneriva- ja transmissioonelektronmikroskoobiga millega analüüsiti nendes esinenud Ca-fosfaatsete struktuuride suurusi ja morfoloogiat. Noodulitele arvutati korrigeeritud suurusjaotus, eeldades, et noodulid olid algselt sfäärilised ja ei ole omavahel lõikuvad.

Fosfaat on proovides kontsentreerunud noodulitesse, läätsedesse ja mikrokihtidesse. Noodulid on ca 100-2700 μm suurused, osalt peaaegu sfäärilised, osalt lamendunud ning esinevad isoleeritult, kettidena või kihtidena. Suuruse, morfoloogia, tafonoomia ja tekkekeskkonna poolest sarnanevad need noodulid tänapäevaste *Thiomargarita* perekonna väävlibakteritele. Tekkemehhanismiks on pakutud lagunenud tsütoplasmaga, kuid säilinud limakapsliga

bakterite sisemuse koloniseerimist teiste mikroorganismide poolt, kes hiljem ise mineraliseerusid, säilitades nooduli kuju.

Noodulid ja läätsed koosnevad ca 1-8 μm pikkuste silindriliste apatiidiosakeste massist. Neil osakestel võib täheldada mitmeid säilivusstaadiume. Vähem ümberkristalliseerunud silindrilistel osakestel on Ca-fosfaadist ja süsinikurikkast materjalist koosnev heterogeenne sisemus, mida ümbritseb homogeensetest, korrastatud apatiidi kristalliitidest koosnev ääris. Enamasti on osakesed aga täielikult ümberkristalliseerunud heksagonaalseteks apatiidi kristallideks, kusjuures osakeste tuumades leidub hulgaliselt suletisi.

Püsivad suurused ja kujud, esinemisrohkus, siseehituse keerukus, säilivustüübid ja tekkekeskkond on tõendid tõlgendusele, et silindrid on ANME-1 sarnaste metanotroofsete arhede mineraliseerunud fossiilid. Mineralisatsioon sai tõenäoliselt alguse rakumembraanile heterogeenselt nukleerunud apatiidi kristalliitidest, mis pärast organismi surma hakkasid diageneetilises keskkonnas kasvama ja ühinema, täites lõpuks kogu silindri sisemuse.

Lihtlitsents lõputöö reprodutseerimiseks ja lõputöö üldsusele kättesaadavaks tegemiseks

Mina,_____Kaarel Mänd_____
(*autori nimi*)

(sünnikuupäev: _____12. mai 1991_____)

1. annan Tartu Ülikoolile tasuta loa (lihtlitsentsi) enda loodud teose
_____Morphology and structure of putative fossilized phosphatic_____
_____sulfur-bacteria and methanotrophic archea in 2.0 Ga old_____
_____organic-rich mudstones, Zaonega formation_____
(*lõputöö pealkiri*)

mille juhendaja on _____Kalle Kirsimäe_____,
(*juhendaja nimi*)

1.1. reprodutseerimiseks säilitamise ja üldsusele kättesaadavaks tegemise eesmärgil, sealhulgas digitaalarhiivi DSpace-is lisamise eesmärgil kuni autoriõiguse kehtivuse tähtaja lõppemiseni;

1.2. üldsusele kättesaadavaks tegemiseks Tartu Ülikooli veebikeskkonna kaudu, sealhulgas digitaalarhiivi DSpace´i kaudu kuni autoriõiguse kehtivuse tähtaja lõppemiseni.

2. olen teadlik, et punktis 1 nimetatud õigused jäävad alles ka autorile.

3. kinnitan, et lihtlitsentsi andmisega ei rikuta teiste isikute intellektuaalomandi ega isikuandmete kaitse seadusest tulenevaid õigusi.

Tartus, 24.05.2013